activity of fibroblast growth factors (11). Based on these findings, we have demonstrated in our previous work using X-ray photoelectron spectroscopy that polyphosphoric acid (PPA) can be tightly adsorbed to the Ti surface in a dose-dependent manner (12). In addition, we reported that a Ti surface treated with PPA significantly enhanced initial attachment and proliferation of two types of cells, namely, human bone marrow-derived mesenchymal stem cells and mouse osteoblast-like cells (12, 13). We could demonstrate that these accelerated cell responses were not due to increased surface roughness induced by PPA, but rather must be ascribed to the biological effect of PPA itself (12). In this way, treatment of Ti with PPA might be a new methodology to fabricate bioactive Ti implants.

In order to assess the potential promoting effect of this Ti surface modification on bone regeneration around implants, we have now carried out an *in vivo* study using a rat model. The study was conducted to compare the bone-implant contact ratio (BICR) of Ti implants treated with three different concentrations (0, 1 and 10 wt%) of PPA. The null hypothesis tested in this study was that there is no difference in BICR amongst Ti implants treated with the three differently concentrated PPA solutions.

Materials and methods

Animal

Eight-week-old-male Wister rats (n = 30) were housed in a temperature-controlled room with a 12-h alternating light-dark cycle and were given water and food *ad lib* throughout the study. The Animal Care Use Review Committee of the Okayama University Dental School approved the experimental protocol in this study (OK-2006314).

Titanium implant surface treatment

Commercially available pure Ti cylinders* (Grade-II; 2 mm in diameter, 4 mm in length) were used in this study. As shown in Fig. 1, part of the cylinder was narrowed to a diameter of 1 mm. The Ti cylinders were first cleaned by ultrasonic rinsing successively in trichloroethylene and ethanol (10 min each). They were then immersed in two different solutions of PPA† with concentrations of 1 and 10 wt% for 24 h at 37 °C. Ti cylinders cleaned and immersed in distilled water for 24 h at 37 °C served as control. After each surface treatment, each cylinder was washed three times with distilled water (PPA is very soluble in water and any unreacted acid is therefore easily removed) and autoclaved.

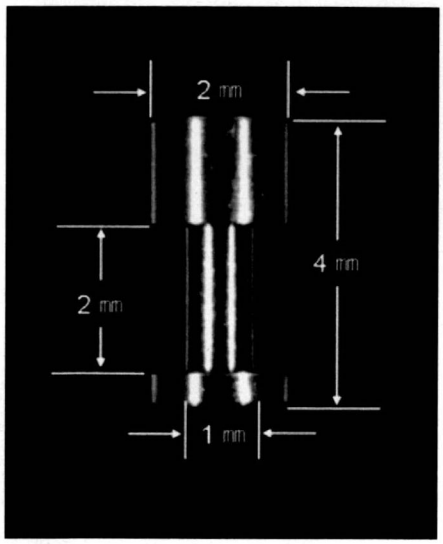

Fig. 1. The titanium implant utilized in this study.

Implantation

The animals were anaesthetized using ketamine hydrochloride (35 mg kg^{-1}) and xylazine hydrochloride (12 mg kg^{-1}). Both the tibiae were shaved and disinfected, and a full thickness incision was made on the dorsal aspect of the tibiae. Implants sites were drilled under cooled sterile saline irrigation using a twist drill‡ (diameter of 2·0 mm). The three differently treated Ti cylinders were randomly implanted into the prepared holes in the tibiae (n = 20 per experimental group). The wound was then sutured. The rats were allowed to recover and were housed as described above.

Section preparation

Two or four weeks after operation, the animals were deeply anaesthetized with diethyl ether and perfused through the abdominal aorta with physiological saline,

*GC, Tokyo, Japan.
†WAKO, Osaka, Japan.
‡Nobel Biocare AB, Gotenberg, Sweden.

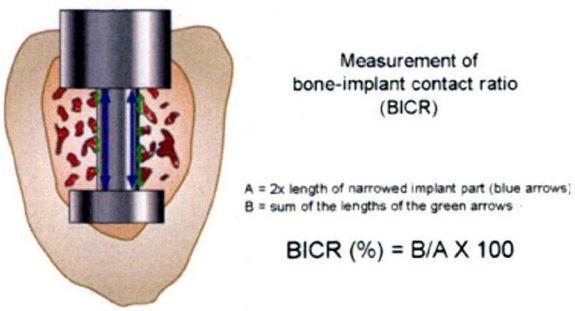

Fig. 2. Schematic drawing explaining the measurement of the bone-implant contact ratio (BICR).

followed by a fixative containing 10% paraformaldehyde and 5% glutaraldehyde in 0·1 M phosphate buffer. After the tibiae were dissected (n = 30 tibiae for each time interval, of which 10 per experimental group), the samples containing the implants were trimmed and immersed in the same fixative for 1 week. The specimens were dehydrated in graded ethanol and styrene, and then embedded in polyester resin, (Rigolac).[§] The embedded materials were polymerized, after which undecalcified sections were ground parallel to the long axis of the implant to a thickness of approximately 70 μm using an ECOMET3 grinding system.[¶]

Histological and histometrical analysis

The sections were double-stained with basic fuchsine and methylene blue, and then imaged by light microscopy (BioZero BZ-8000).** Using the photomicrographs of each section, the BICR of the implant was determined semi-automatically by three examiners blinded to the experimental group using the commercially available BZ Analyzer software** (Fig. 2). As shown in Fig. 2, the BICR was evaluated only in the narrow portion of the implant. Mean BICR data determined by three examiners were calculated in each section and submitted for statistical analysis. The statistical analysis was performed using one-way ANOVA followed by Scheffe's multiple comparison tests.

[§]Nissin EM, Tokyo, Japan.
[¶]Buehler, Lake Bluff, IL, USA.
**KEYENCE, Osaka, Japan.

Results

Histological findings

Histological observation of the sections that were prepared 2 weeks after implantation revealed that new bone formation was observed in direct contact with the Ti surface in all the experimental conditions. Additionally, bone trabeculae with a mesh-like structure were seen in the medullary canal (Fig. 3, arrows). Those bone trabeculae in the PPA-treated Ti implants were somewhat denser than those in the control untreated Ti implants. However, those mesh-like structures tended to disappear 4 weeks after implantation in all the experimental conditions (Fig. 4). With regard to the newly formed bone trabeculae at the interface between Ti and medulla, those in the PPA-treated groups seemed abundant, both 2 and 4 weeks after implantation. Especially, 4 weeks after implantation, consecutive bone trabeculae formation was observed in the PPA-treated Ti implant groups (Fig. 4).

Histometrical findings

Regarding BICR analysis, statistics revealed that PPA treatment of the Ti implant surface significantly enhanced direct bone contact to the Ti surface. Especially the BICRs of the 1 wt% PPA-treated Ti implants were significantly higher than those of the control untreated Ti implants, both 2 and 4 weeks after implantation (Fig. 5). At the latter observation period, the mean BICR of the 10 wt% PPA treatment implants was also significantly higher than that of the untreated Ti implants.

Discussion

In this study, we utilized Ti cylinders with the major middle part narrowed. We then quantified the amount of bone formation along the vertical axis of the implant, but only at the narrowed area. When such a Ti cylinder was implanted into the prepared hole in the tibia, the area around the narrowed implant part got filled with a blood clot so that there was no direct contact with cancellous bone. As cancellous bone involves abundant bone-related cells (e.g. osteoblasts, mesenchymal stem cells), we prevented in this way that such bone-related cells would directly attach to and proliferate on the adjacent Ti surface (osseointegration). Therefore, this

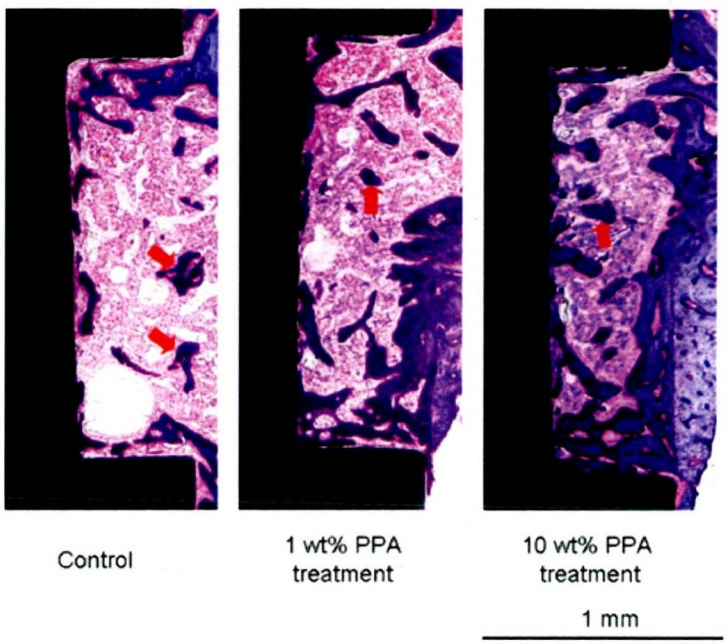

Fig. 3. Representative histological images of sections through the bone-implant interface 2 week after implantation. Bone trabeculae with mesh-like structures (arrows) were seen in the medullary canal in all experimental conditions. The newly formed bone trabeculae in contact with the Ti surface tended to be thicker when the Ti surface was treated with polyphosphoric acid (PPA).

model allowed us to evaluate the effect of PPA treatment of the Ti surface on bone regeneration around the implant.

Two weeks after implantation, new bone formation in direct contact with the Ti surface was observed in all the experimental conditions. Furthermore, bone with a mesh-like structure was clearly present in the medullary canal. These trabeculae most likely result from the inflammatory response to the implantation. The bone trabeculae around the PPA-treated Ti implants were somewhat thicker than those around the control untreated Ti implants. Four weeks after implantation, most mesh-like bone structures disappeared in all the experimental conditions. These findings are consistent with other previous reports (14, 15).

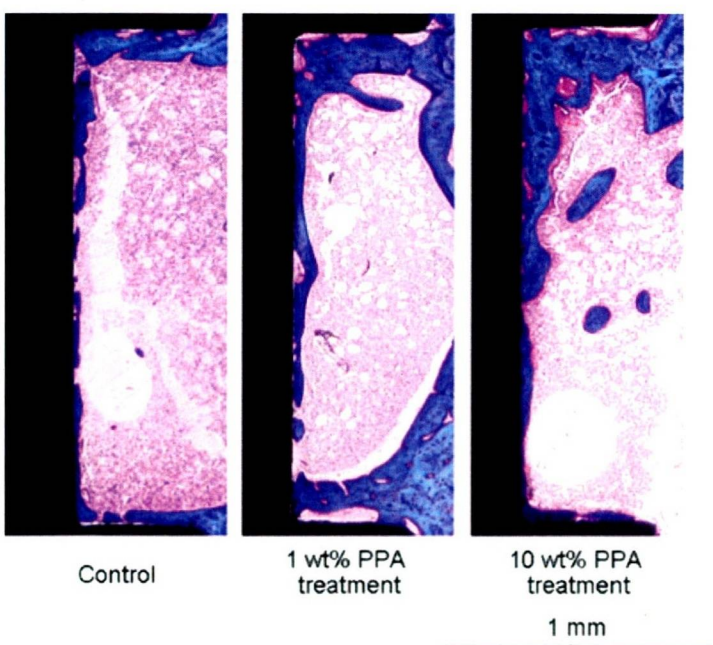

Fig. 4. Representative histological images of sections through the bone-implant interface 4 week after implantation. The bone trabeculae with mesh-like structures that were observed in the medullary canal 2 weeks after implantation, disappeared at this stage. Two weeks after implantation, the newly formed bone trabeculae in contact with the Ti surface tended to be thicker when the Ti surface was treated with polyphosphoric acid (PPA).

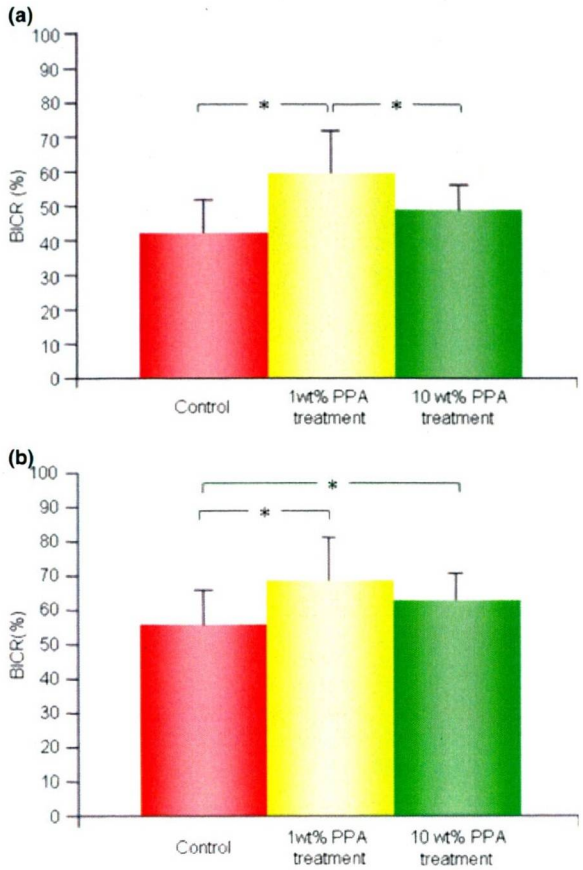

Fig. 5. The mean bone-implant contact ratio (BICR) of the untreated and treated Ti implants 2 and 4 weeks after implantation (n = 10 for each condition). (a) The mean BICR 2 weeks after implantation. The mean BICR of the 1 wt% polyphosphoric acid (PPA)-treated Ti implants was significantly higher than that of the untreated control and the 10 wt% PPA-treated Ti implants 2 weeks after implantation. (b) The mean BICR 4 weeks after implantation. Although 4 weeks after implantation, the mean BICR of the 1 wt% PPA-treated Ti implants was the highest, both the 1 and 10 wt% PPA treatment resulted in a significantly higher mean BICR than that of the untreated Ti implants in control. *Indicates statistical significance ($P < 0{\cdot}05$).

Regarding BICR, PPA treatment of the Ti implant surface significantly enhanced the amount of direct bone contact to the Ti surface. Especially, the BICR of 1 wt% PPA-treated Ti implants was significantly higher than that of the control Ti implants, both 2 and 4 weeks after implantation. At 4 weeks, 10 wt% PPA treatment also significantly increased the BICR as compared to the BICR of the control Ti implants. Such early and abundant bone formation surrounding an implant must contribute to the implant stability. Hence, surface treatment of Ti implants with PPA was shown to be an effective method to modify the Ti surface for improved osseoconductiveness.

This enhanced bone formation around PPA-treated Ti implants must most likely be ascribed to an accelerated cell response to PPA that was adsorbed on the Ti implant surface, as we demonstrated before using X-ray photoelectron spectroscopy (12). Our previous *in vitro* research also revealed that PPA bound to the Ti surface induced several biological effects on cultured cells (12, 13). More specifically, proliferation of human mesenchymal stem cells as well as mouse osteoblast-like cells was found to have extremely accelerated PPA-treated Ti surfaces in a dose-dependent manner. Nevertheless, some contradiction exists between the results of our previous *in vitro* cell culture data and our current *in vivo* BICR data. While a higher concentration of PPA resulted in a more accelerated cell proliferation, the BICR data in this study indicated that the 1 wt% PPA treatment was superior to the highly concentrated (10 wt%) PPA treatment. On the other hand, the newly formed bone trabeculae that contacted the Ti surface tended to be thicker when the cylinders were treated with PPA and this phenomenon seemed most obvious for the 10 wt% PPA treatment. Like BICR, the thickness of the bone trabeculae may also contribute to the implant stabilization in order to distribute masticatory and other oral stress. Therefore, also measurement of the bone trabeculae thickness might be a useful index to assess the effect of Ti surface treatments on bone regeneration in search for clinically useful bioactive implants.

In summary, the present *in vivo* data that PPA treatment of the Ti surface lead to more abundant bone formation in contact with the implant suggests that this method may shorten the healing period after implant placement. From a clinical point of view, this PPA surface treatment may be advantageous as compared to methods that coat the Ti surface with various bioactive substances. As most of these bioactive substances are proteins, careful attention is needed not to lose their biological activity before implant placement. In this way, Ti implant surface modification using PPA is simple and does not need special handling afterwards. For further development of this PPA treatment of Ti implants towards clinical application, more studies are definitely needed to determine the most optimal PPA treatment conditions that induce the rapidest and most abundant bone

formation around the implant, especially using animals that are closely related to human beings (e.g. beagle dogs, monkeys).

Acknowledgments

This study was supported in part by a Grant-in-Aid for Scientific Research from the Ministry of Education, Science, Sports and Culture of Japan (#17390516).

References

1. Cooper LF. A role for surface topography in creating and maintaining bone at titanium endosseous implants. J Prosthet Dent. 2000;84:522–534.
2. Rupp F, Scheideler L, Rehbein D, Axmann D, Geis-Gerstorfer J. Roughness induced dynamic changes of wettability of acid etched titanium implant modifications. Biomaterials. 2004;25:1429–1438.
3. Rupp F, Scheideler L, Olshanska N, De Wild M, Wieland M, Geis-Gerstorfer J. Enhancing surface free energy and hydrophilicity through chemical modification of microstructured titanium implant surfaces. J Biomed Mater Res A. 2006;76:323–334.
4. Kim MJ, Kim CW, Lim YJ, Heo SJ. Microrough titanium surface affects biologic response in MG63 osteoblast-like cells. J Biomed Mater Res A. 2006;79:1023–1032.
5. Shalabi MM, Gortemaker A, Van't Hof MA, Jansen JA, Creugers NH. Implant surface roughness and bone healing: a systematic review. J Dent Res. 2006;85:496–500.
6. Sul YT, Johansson C, Albrektsson T. Which surface properties enhance bone response to implants? Comparison of oxidized magnesium, TiUnite, and Osseotite implant surfaces Int J Prosthodont. 2006;19:319–328.
7. Hayakawa T, Yoshinari M, Nemoto K. Direct attachment of fibronectin to tresyl chloride-activated titanium. J Biomed Mater Res A. 2003;67:684–688.
8. Park JM, Koak JY, Jang JH, Han CH, Kim SK, Heo SJ. Osseointegration of anodized titanium implants coated with fibroblast growth factor-fibronectin (FGF-FN) fusion protein. Int J Oral Maxillofac Implants. 2006;21:859–866.
9. Hilbig H, Kirsten M, Rupietta R, Graf HL, Thalhammer S, Strasser S *et al.* Implant surface coatings with bone sialoprotein, collagen, and fibronectin and their effects on cells derived from human maxillar bone. Eur J Med Res. 2007;12:6–12.
10. Liu Y, Enggist L, Kuffer AF, Buser D, Hunziker EB. The influence of BMP-2 and its mode of delivery on the osteoconductivity of implant surfaces during the early phase of osseointegration. Biomaterials. 2007;28:2677–2686.
11. Shiba T, Nishimura D, Kawazoe Y, Onodera Y, Tsutsumi K, Nakamura R *et al.* Modulation of mitogenic activity of fibroblast growth factors by inorganic polyphosphate. J Biol Chem. 2003;278:26788–26792.
12. Maekawa K, Yoshida Y, Mine A, Fujisawa T, Van Meerbeek B, Suzuki K *et al.* Chemical interaction of polyphosphoric acid with titanium and its effect on human bone marrow derived mesenchymal stem cell behavior. J Biomed Mater Res A. 2007;82:195–200.
13. Maekawa K, Yoshida Y, Mine A, Van Meerbeek B, Suzuki K, Kuboki T. Effect of polyphosphoric-acid pre-treatment of titanium on attachment, proliferation and differentiation of osteoblast like cells (MC3T3-E1). Clin Oral Implants Res. 2008;19:320–325.
14. Takeshita F, Morimoto K, Suetsugu T. Tissue reaction to alumina implants inserted into the tibiae of rats. J Biomed Mater Res. 1993;27:421–428.
15. Ayukawa Y, Okamura A, Koyano K. Simvastatin promotes osteogenesis around titanium implants. Clin Oral Implants Res. 2004;15:346–350.

Correspondence: Takuo Kuboki DDS, PhD, Professor and Chair, Department of Oral Rehabilitation and Regenerative Medicine, Okayama University Graduate School of Medicine and Dentistry and Pharmaceutical Sciences, 2-5-1 Shikata-cho, Okayama 700-8525, Japan.
E-mail: kuboki@md.okayama-u.ac.jp

J. Biochem. 2009;145(2)207–216
doi:10.1093/jb/mvn159

CCN Family 2/Connective Tissue Growth Factor Modulates BMP Signalling as a Signal Conductor, Which Action Regulates the Proliferation and Differentiation of Chondrocytes

Azusa Maeda[1,2], Takashi Nishida[1], Eriko Aoyama[3], Satoshi Kubota[1], Karen M. Lyons[4], Takuo Kuboki[2] and Masaharu Takigawa[1,*]

[1]Department of Biochemistry and Molecular Dentistry; [2]Department of Oral Rehabilitation and Regenerative Medicine, Okayama University Graduate School of Medicine, Dentistry and Pharmaceutical Sciences, Okayama, Japan; [3]Biodental Research Center, Okayama University Dental School, Okayama, Japan; and [4]Department of Orthopaedic Surgery, David Geffen School of Medicine at UCLA, CA, USA

Received September 9, 2008; accepted November 17, 2008; published online November 27, 2008

Both CCN family 2/connective tissue growth factor (CCN2/CTGF) and bone morphogenetic protein (BMP)-2 play an important role in cartilage metabolism. We evaluated whether or not CCN2 would interact with BMP-2, and examined the combination effect of CCN2 with BMP-2 (CCN2-BMP-2) on the proliferation and differentiation of chondrocytes. Immunoprecipitation-western blotting analysis, solid-phase binding assay and surface plasmon resonance (SPR) spectroscopy showed that CCN2 directly interacted with BMP-2 with a dissociation constant of 0.77 nM as evaluated by SPR. An *in vivo* study revealed that CCN2 was co-localized with BMP-2 at the pre-hypertrophic region in the E18.5 mouse growth plate. Interestingly, CCN2-BMP-2 did not affect the BMP-2/CCN2-induced phosphorylation of p38 MAPK but caused less phosphorylation of ERK1/2 in cultured chondrocytes. Consistent with these results, cell proliferation assay showed that CCN2-BMP-2 stimulated cell growth to a lesser degree than by either CCN2 or BMP-2 alone, whereas the expression of chondrocyte marker genes and proteoglycan synthesis, representing the mature chondrocytic phenotype, was increased collaboratively by CCN2-BMP-2 treatment in cultured chondrocytes. These findings suggest that CCN2 may regulate the proliferating and differentiation of chondrocytes by forming a complex with BMP-2 as a novel modulator of BMP signalling.

Key words: chondrocytes, CCN family 2/connective tissue growth factor (CCN2/CTGF), BMP signalling, BMP-2, endochondral ossification.

Abbreviations: E, embryonic day; ECM, extracellular matrix; ERK1/2, extracellular signal-regulated kinase 1/2; HA, influenza virus hemagglutinin; His, histidine; MAPK, mitogen-activated protein kinase; phospho, phosphorylation; rCCN2, recombinant CCN2 protein; WT, wild type.

INTRODUCTION

Endochondral ossification is initiated by the condensation of mesenchymal cells and the subsequent differentiation of them into chondrocytes within the condensates (*1*, *2*). Chondrocytes proliferate and produce many kinds of extracellular matrix (ECM) molecules characteristic of cartilage, such as type II collagen, aggrecan, link proteins and hyaluronate (*1*, *2*). Once embedded in ECM, these cells differentiate into pre-hypertrophic and hypertrophic chondrocytes (*1*, *2*). Hypertrophic chondrocytes, in which cell growth is arrested, eventually mineralize the surrounding matrices, allowing the invasion of blood vessels and osteoblasts (*1*, *2*). Finally, the cartilage is replaced by bone. In this differentiation process, a number of growth factors, such as transforming growth factor (TGF)-β (*3*), insulin-like growth factor (IGF, *4*), bone morphogenetic proteins (BMPs, *5*) and CCN family 2/connective tissue growth factor (CCN2) have been implicated (*6*). Among them, CCN2 is highly expressed in the pre-hypertrophic region of growth plate (*6*). As a member of the CCN family, it consists of four distinct structural modules, i.e. insulin-like growth factor binding protein-like (IGFBP), von Willebrand type C repeat (VWC), thrombospondin type 1 repeat (TSP1) and carboxy-terminal cysteine knot (CT). Also, CCN2 promotes multiple steps of the endochondral ossification, such as proliferation, maturation and hypertrophy of chondrocytes (*6*, *7*). In addition, we reported earlier that CCN2 functions to maintain the integrity of the cartilage tissues *in vivo* (*8*). These findings suggest that CCN2 plays a very important role in chondrocyte metabolism. In fact, it has been reported that *Ccn2*-deficient mice die soon after birth, as a result of, at least in part, severe skeletal abnormalities associated with impaired endochondral ossification (*9*). These and other findings indicate that CCN2 is an essential growth factor for regulation of the proliferation, maturation and hypertrophy of chondrocytes (*7*, *9*). Recently, it was reported that CCN2 interacted with many growth factors critically

*To whom correspondence should be addressed. Tel: +81-86-235-6645, Fax: +81-86-235-6649,
E-mail: takigawa@md.okayama-u.ac.jp

involved in cartilage metabolism, such as TGF-β, BMP-4 (*10*), and vascular endothelial growth factor (VEGF, *11*) and that CCN2 modified the activity of each growth factor. Therefore, CCN2 may control the network of growth factors during endochondral ossification; and thus it may be called a 'signal conductor' with novel functions.

BMP-2 is also a multifunctional growth factor, and it was originally defined by its ability to induce ectopic bone and cartilage formation *in vivo* (*12*). Although it was reported that BMP-2 promoted the proliferation, maturation and hypertrophy of chondrocytes *in vitro* (*5*, *13*, *14*), newborn transgenic mice, in which Bmp-2 had been inactivated in a limb-specific manner, had normal skeletons (*15*). These findings suggest that other BMPs present in the developing limb can compensate for the loss of BMP-2. Until now, more than 30 BMP family members have already been described, and they have been classified into several subgroups according to their structural similarities (*16*). In particular, BMP-2 and BMP-4 are highly related molecules, and both molecules have potent bone-forming activity (*17*). These findings indicate that the functions of BMP-2 and BMP-4 are interchangeable during bone formation in the limb. In fact, it was reported that the loss of both BMP-2 and BMP-4 in a limb-specific manner resulted in a delay in cartilage development and in a severe impairment of osteogenesis (*18*). Furthermore, the BMP receptor type 1A (Bmpr1a), BMP receptor type 1B (Bmpr1b) double-deficient mice exhibited severe defects in chondrogenesis and osteogenesis (*19*). Taken together, these results suggest that BMP signalling is essential for endochondral ossification, and that BMP-2 and BMP-4 compensate each other to transduce sufficient BMP signalling to allow cartilage cells to differentiate.

Although it has been already reported that CCN2 interacts with BMP-4 and inhibits the action of BMP-4 in early embryonic patterning (*7*), investigation of the interaction of CCN2 with BMP-2 as well as BMP-4 may reveal the novel function of CCN2 in BMP signalling required for cartilage development. Therefore, we investigated whether or not CCN2 directly interacts with BMP-2 and examined the combinational effect of CCN2 with BMP-2 on chondrocyte proliferation and differentiation. In this study, we demonstrated that CCN2 directly interacted with BMP-2 and promoted CCN2/BMP-2-induced proteoglycan synthesis, whereas proliferation of chondrocytes was interfered with the combination. These findings suggest that CCN2 has both antagonistic effect and agonistic effect on BMP-2.

MATERIALS AND METHODS

Materials—Dulbecco's modified Eagle's medium (DMEM), α-modification of Eagle's medium (αMEM), and fetal bovine serum (FBS) were purchased from Nissui Pharmaceutical (Tokyo, Japan), ICN Biomedicals (Aurora, OH), and Cancera International (Rexcalale, ON, Canada), respectively. Plastic dishes and multiwell plates were obtained from Greiner Bio-One (Frickenhausen, Germany). Hybond-N membrane and [α-^{32}P]dCTP (specific activity: 110 TBq/mmol) were from GE Healthcare UK (Little Chalfont, United Kingdom), and [^{35}S]sulfate (37 MBq/ml) was from PerkinElmer (Waltham, MA). Hyaluronidase and anti-β-actin were obtained from Sigma (St Louis, MO). Anti-phospho-extracellular signal-regulated kinase (ERK)1/2, and anti-phospho-p38 were from Promega (Madison, WI); and anti-ERK1/2, anti-p38, and anti-phospho-Smad1/5/8, from Cell Signalling Technology (Beverly, MA). Anti-BMP-2 was purchased from R & D Systems (Minneapolis, MN); and anti-HA, from Covance (Princeton, NJ). Anti-CCN2 serum was raised in rabbits, and recombinant CCN2 (rCCN2) was purified as previously reported (*20*). For binding assays and surface plasmon resonance (SPR) analysis, polyhistidine (His)-tagged rCCN2 and each of the four modules of the CCN2 were purchased from Biovendor (Heidelberg, Germany), or were produced by *Escherichia coli* harbouring the corresponding expression plasmids. Recombinant BMP-2 (rBMP-2) was kindly provided by Dr K. Sugama of Osteopharma (Osaka, Japan).

Animals—BalbC/129sv hybrid CCN2$^{+/-}$ mice were crossbred to obtain wild-type (WT) and *Ccn2*-deficient mice, which were used at E18.5 (*9*). These mice were euthanized to obtain the rib cage for cell culture and the metatarsal bone with surrounding tissues for immunostaining. All mice were genotyped by using PCR. The Animal Committee of Okayama University Graduate School of Medicine, Dentistry, and Pharmaceutical Sciences approved all of the procedures.

Cell Culture—Cells of the human chondrosarcoma-derived cell line HCS-2/8 (*21*) were inoculated at a density of 4×10^4 cells/cm^2 into 96-well or 24-well multiplates containing DMEM supplemented with 10% FBS and were cultured at 37°C under 5% CO_2 in air. Primary cultures of chondrocytes isolated from the ventral half of the rib cages of E18.5 mouse embryos were prepared as described previously (*22*). The isolated chondrocytes were seeded at a density of 1×10^5 cells/cm^2 into 3.5 cm dishes in αMEM containing 10% FBS and were then cultured at 37°C under 5% CO_2 in air.

Western Blot Analysis—HCS-2/8 cells were transfected with a CCN2 expression plasmid with an HA-tag by using Fugene6 reagent (Roche, Basel, Switzerland). After 2 days, the cell lysate was collected, and immunoprecipitation was performed with anti-BMP-2 antibody. Then, the HA-tagged CCN2 was detected in the immunoprecipitated sample by western blotting by using an anti-HA antibody. Western blot analysis was performed as described previously (*23*).

Solid-Phase Binding Assay—A 96-well multiplate was pre-coated with rBMP-2 (0.3–10 μg/ml) at 4°C overnight. Then, rCCN2 with a His-tag was added to each well, and incubation was carried out at 4°C for 6 h. After washing each well, we measured the optical absorbance (450 nm) representing the binding of CCN2 to BMP-2 by conducting a colorimetric assay using the anti-His antibody.

Immunohistochemistry—Mouse metatarsal bones with surrounding tissues were dissected and fixed in 10% formalin overnight at 4°C before being embedded in paraffin. Five micrometre sections were mounted on glass slides, deparaffinized and treated with hyaluronidase (25 mg/ml) for 30 min at room temperature. Immunohistochemistry was performed with a Histofine kit

(Nichirei; Tokyo, Japan) as described previously (*23*). Colour was developed with diaminobenzidine (DAB), and sections were counterstained with methyl green. The proliferative population of chondrocytes in growth cartilage tissues was determined using a commercial proliferating cell nuclear antigen (PCNA) staining kit (Zymed laboratories, Carlsbad, CA), following the manufacturer's instructions.

Evaluation of Proteoglycan Synthesis—Mouse costal chondrocytes or HCS-2/8 cells were grown to subconfluence in 24-well multiplates containing αMEM or DMEM supplemented with 10% FBS, respectively. Thereafter, the medium was replaced with that containing 0.5% FBS and rCCN2, rBMP-2 or both. [^{35}S]sulfate (37 MBq/ml) dissolved in PBS was added to the culture at a final concentration of 370 kBq/ml at 5 h after the addition of these factors, and incubation was continued for another 17 h. After labelling, the cultures were digested with 1 mg/ml actinase E, and the radioactivity of the material precipitated with cetylpyridinium chloride was measured in a scintillation counter.

Northern Blot Analysis—Total RNAs were prepared by using ISOGEN reagent (Nippon Gene, Tokyo, Japan) from mouse costal chondrocytes stimulated with rCCN2, rBMP-2 or their combination for 6 h. Then, 10 μg of total RNA was subjected to electrophoresis on a 1% formaldehyde-agarose gel and subsequently transferred onto Hybond-N filters (GE Healthcare). Northern blot analysis was performed as described previously (*23*). Specific PCR products of aggrecan cDNA and linearized plasmids containing mouse-type II collagen (*22*), type X collagen (*9*) and Runt domain transcription factor (Runx2/Cbfa1, *24*) cDNAs were used as probes.

Surface Plasmon Resonance Spectroscopy—Specific interaction between CCN2 and BMP-2 was analysed by using a BIAcore X (GE HealthCare). rCCN2 coupling, blocking and regeneration of a CM5 chip were performed according to the manufacturer's protocol. rBMP-2 in HBS-EP buffer (10 mM HEPES, 0.15 M NaCl, 3 mM EDTA and 0.005% Tween 20; pH 7.4) at several concentrations was perfused at a flow rate of 10 μl/min at 25°C over the control surface or a surface bearing immobilized CCN2, and the resonance changes were recorded. The response on the control surface was subtracted from that on the CCN2-conjugated surface. The dissociation constants (K_d) were determined by using BIA evaluation software.

Proliferation Assay—For measurement of cell proliferation, HCS-2/8 cells were inoculated into 96-well multiplates at a density of 1×10^4/well, and then the cells were stimulated with rCCN2, rBMP-2 or their combination for 24 h. Thereafter, the proliferation of these cells was determined by conducting a TetraColor ONE assay according to the recommended protocol (Seikagaku Co. Tokyo, Japan). Briefly, 10 μl of TetraColor ONE solution was added to 100 μl of medium of each culture. After the incubation for up to 4 h at 37°C, the absorbance of culture medium was measured at a wavelength of 450 nm.

Statistical Analysis—Unless otherwise specified, all experiments were repeated at least twice, and similar results were obtained. Statistical analysis was performed by using Student's *t*-test.

RESULTS

Interaction of CCN2 with BMP-2 Through Its CT Domain—It has been reported that CCN2 directly binds to BMP-4 through its VWC module (*10*). Because not only BMP-4 but also BMP-2 plays an important role in chondrocyte proliferation and differentiation during endochondral ossification (*13*, *14*), we investigated the involvement of CCN2 in BMP-2 signalling of chondrocytes. As shown in Fig. 1, we found that CCN2 interacted with BMP-2 similarly as with BMP-4. An HA epitope-tagged construct of full-length CCN2 was generated, and the protein was produced in HCS-2/8 cells. After 2 days, cell lysates were collected and immunoprecipitation was performed with anti-BMP-2 antibody in cell lysate in the presence or absence of rBMP-2. Western blot analysis of the immunoprecipitated samples was performed by using anti-HA antibody. As a result, HA-tagged CCN2 was detected only in the presence of rBMP-2 (Fig. 1A). In addition, to test whether CCN2 directly interacted with BMP-2, or not, we performed a solid-phase binding assay. As shown in Fig. 1B, CCN2 directly bound to BMP-2 in a BMP-2-dependent manner. Subsequently, a binding assay using each recombinant module protein of CCN2 was performed to determine which module was responsible for the binding to BMP-2. As shown in Fig. 1C, the CT module of CCN2 distinctly bound to BMP-2, whereas VWC and IGFBP modules slightly bound to it. To further verify if CT or amino-terminal module plays an important role in binding to BMP-2, we generated a N-terminal IGFBP-VWC and C-terminal TSP1-CT fragments and evaluated their binding ability. As shown in Fig. 1D, while both fragments significantly interacted with BMP-2, interaction of TSP1-CT fragment of CCN2 with BMP-2 was stronger than that of IGFBP-VWC fragment. These results indicate that not only the CT module, but also the IGFBP-VWC modules are responsible for the binding to BMP-2. Furthermore, the binding affinity of CCN2 for BMP-2 was determined by SPR analysis (BIAcore systems). Kinetic measurements using different concentrations of CCN2 yielded a K_d of 0.77 nM for BMP-2 (Fig. 1E). These data indicate that CCN2 can directly bind to BMP-2 through its CT domain.

Co-Localization of CCN2 with BMP-2 in Pre-Hypertrophic Region of the Growth Plate—Growth plate chondrocytes are horizontally organized into distinct zones. The zones reflect the sequential differentiation stages of chondrocyte proliferation, maturation and hypertrophy (Fig. 2A and B). In wild type mice, proliferative and pre-hypertrophic chondrocytes were stained with anti-PCNA antibody, which has been used as a marker for cell proliferation, but the immunoreactivity of PCNA was not observed in the hypertrophic chondrocytes therein (Fig. 2C). These findings suggest that not only proliferative chondrocytes, but also pre-hypertrophic chondrocytes, which are the major CCN2 producer in growth plate, retain proliferative activity. Because it was shown that CCN2 directly bound to BMP-2 *in vitro*, we investigated whether or not CCN2 was co-localized with BMP-2 in the growth plate using an immunohistochemical analysis with anti-CCN2 and anti-BMP-2 antibodies in E18.5 WT and *Ccn2*-deficient metatarsal growth plates. As shown in Fig. 2G and H,

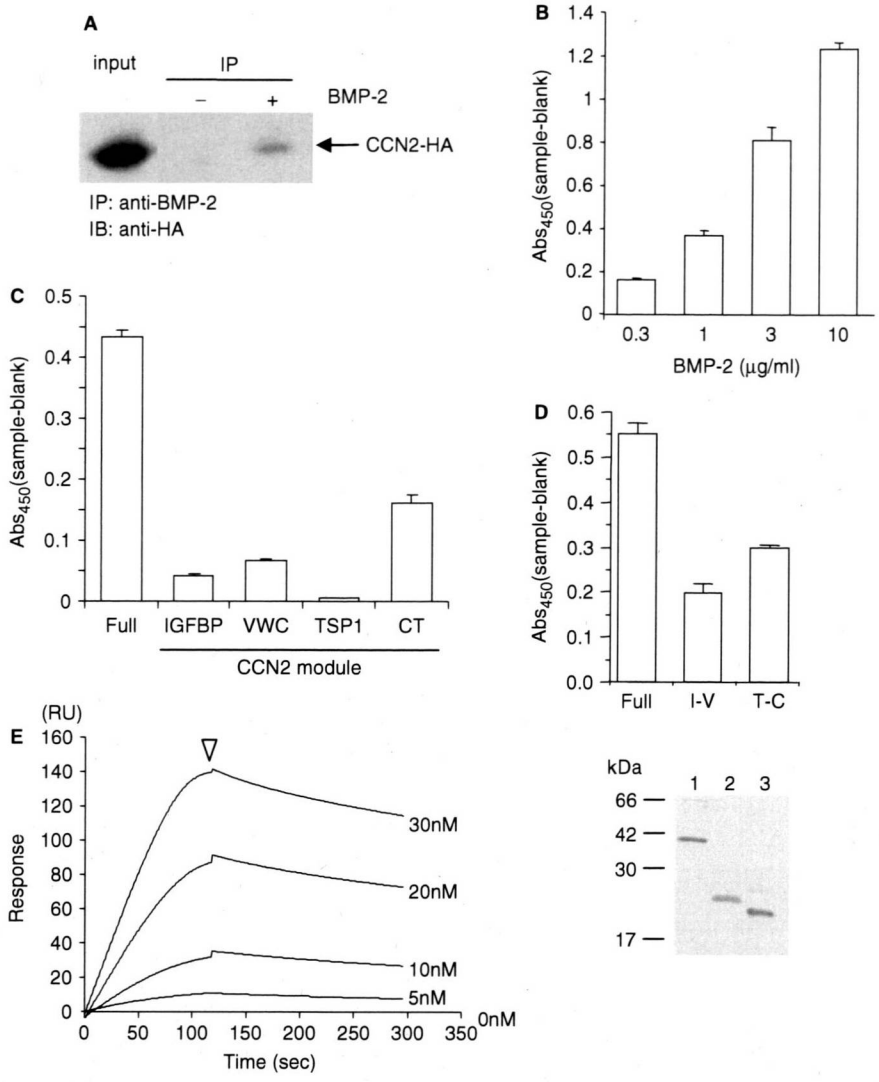

Fig. 1. **Complex formation between CCN2 and BMP-2.** (A) Western blot analysis of CCN2 binding to rBMP-2 after immunoprecipitation with anti-BMP-2. HCS-2/8 cells were inoculated at a density of 5×10^5/well into a 6-well plate; and the next day, the cells were transfected with a CCN2 expression plasmid containing an HA tag. After 2 days, the cell lysates were collected and incubated with or without 1 μg rBMP-2 at 4°C overnight. Then, immunoprecipitaion was performed with anti-BMP-2 antibody at 4°C. After 24 h, the immunocomplexes were captured by adding agarose-protein G beads. The beads were washed, and precipitates were subjected to SDS-PAGE and western blotting with anti-HA antibody. Representative results for total cell lysate (input) and treatment without rBMP-2 (–) and with rBMP-2 (+) are shown. The arrow indicates the signal for CCN2-HA. (B) Solid-phase binding assay for binding of full-length CCN2 to rBMP-2. Ninety-six multiplate wells pre-coated with different concentrations of rBMP-2 (0.3, 1, 3 and 10 μg/ml) were incubated with 6 × His-tagged rCCN2 (500 ng/ml) at 4°C for 6 h. Total binding was determined by measuring immunoreactivity towards the His-tag. Background binding was determined by measuring the immunoreactivity towards the His-tagged CCN2 in the wells pre-coated with BSA at the same concentration of each rBMP-2. Data were calculated by the subtracting background binding from the total binding. Data represents mean ± SD of triplicate samples. (C) Solid-phase binding assay for measuring the binding of each CCN2 module to rBMP-2. CCN2 or its modules (25 μM) were incubated in the wells pre-coated with rBMP-2 at 4°C for 6 h. Bound proteins were determined under the same conditions as in 'B'. Data are presented as the mean ± SD of triplicate samples. (D) Solid-phase binding assay for the evaluation of the binding of IGFBP-VWC or TSP1-CT fragment of CCN2 to rBMP-2. (Upper panel) Full-length CCN2, IGFBP-VWC or TSP1-CT fragment (1 μg/ml) was incubated in the wells pre-coated with rBMP-2 (3 μg/ml) at 4°C for 6 h. Bound proteins were determined under the same conditions as in 'B'. Data are presented as the mean ± SD of triplicate samples. (Lower panel) Recombinant full-length CCN2, IGFBP-VWC and TSP1-CT fragment were separated by SDS–PAGE and visualized by coomassie brilliant blue (CBB) staining. (E) Determination of the binding affinity of rBMP-2 for CCN2 by SPR analysis. Four different concentrations of rBMP-2 ranging between 5 nM and 30 nM were passed through the immobilized CCN2 on the CM5 sensor chip (Time 0 s), and kinetic experiments were performed. After the rBMP-2 flow was stopped (arrowhead), dissociation was monitored by a decrease in the resonance units.

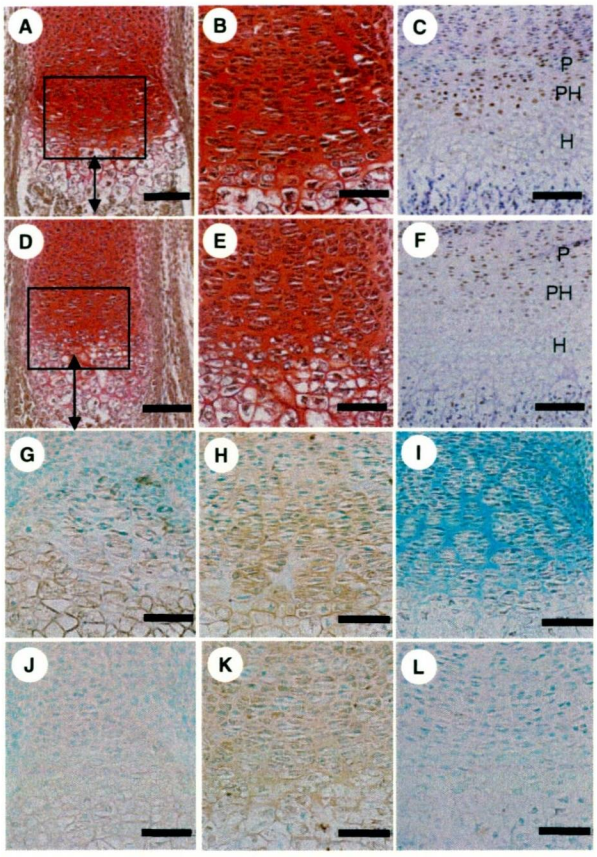

Fig. 2. **Co-localization of CCN2 and BMP-2 in the growth plate of wild-type and *Ccn2*-deficient metatarsal bones.** Sections of the growth plates of E18.5 metatarsal bone (A, B, D, E, G–L) and femur (C, F) in wild-type (A–C, G–I) and *Ccn2*-deficient (D–F, J–L) littermates were stained with safranin-O (A, B, D, E), and immunostained with anti-PCNA antibody (C, F), anti-CCN2 antibody (G, J), anti-BMP-2 antibody (H, K) or normal rabbit IgG as a negative control (I, L). The primary antibodies were visualized by immunoperoxidase, and then the sections were counterstained with methyl green (G–L) or hematoxylin (C, F). Panels 'A' and 'D' are low-power magnification views of the growth plate, and panels 'B, G–I' and 'E, J–L' show high-power magnification of the area delimited by black square in 'A' and 'D', respectively. Bidirectional arrows indicate the length of the hypertrophic zones (A, D). In the wild type, immunostaining with PCNA was detected from proliferative to pre-hypertrophic zone (C), and both CCN2 and BMP-2 were mainly localized in the pre-hypertrophic zone of the growth plate (G, H). In the *Ccn2*-deficient mice, signals for immunoreactivity of PCNA were decreased compared with wild type (F), and CCN2 immunostaining was not detected (J). Signals for immunoreactivity to BMP-2 were located in the proliferative zone (K). Bars in 'A and D' and in 'B, C, E, F and G–L' represent 100 μm and 50 μm, respectively.

both CCN2 and BMP-2 were localized in pre-hypertrophic region of the growth plate, thus suggesting that CCN2 might interact with BMP-2 *in vivo*. On the other hand, as also shown in Fig. 2D–F, J–L, and consistent with previous studies (*9*), an enlarged hypertrophic zone and reduced PCNA signal and safranin-O staining were seen in the growth plate in *Ccn2*-deficient compared with

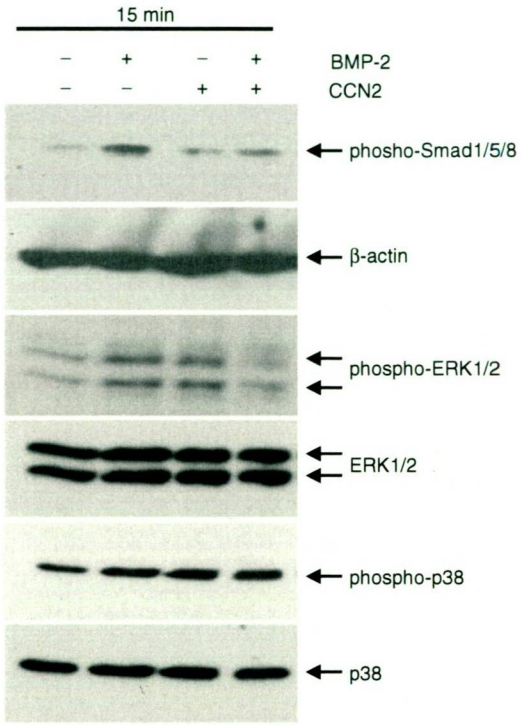

Fig. 3. **Combinational effect of CCN2 and BMP-2 on the activation of Smad1/5/8 and MAPK pathways in mouse chondrocytes.** After the first passage, mouse chondrocytes were cultured in 3.5 cm dishes until they had become subconfluent. Then, the cells were stimulated with 50 ng/ml rBMP-2, 100 ng/ml rCCN2 or the combination of CCN2 (100 ng/ml) and rBMP-2 (50 ng/ml) for 15 min. The mixture of CCN2 with BMP-2 was prepared 2 h before stimulation and was kept on ice to allow hetero complex formation. Cell lysates were collected, and western blot analysis was performed with anti-phospho-Smad1/5/8, anti-β-actin, anti-phospho-ERK1/2, anti-ERK1/2, anti-phospho-p38 and anti-p38 antibodies. The band of phospho-Smad1/5/8 was increased in cells treated with rBMP-2, and the bands of both phospho-ERK1/2 and phospho-p38 were increased in the cells treated with rCCN2 or rBMP-2 after 15 min of treatment. Note that combination of CCN2 and BMP-2 decreased the activation of phospho-Smad1/5/8 and phospho-ERK1/2 but not that of phospho-p38.

that in WT littermates; and as expected, immunoreactivity for CCN2 was not detected (Fig. 2J). Signals indicating immunoreactivity for BMP-2 were detected in chondrocytes in the proliferative cell layer, but not in the pre-hypertrophic zone (Fig. 2K). This pattern of BMP-2 distribution in the *Ccn2*-deficient mice was significantly altered from that in the WT mice. These findings suggest that CCN2 regulates the localization of BMP-2 during endochondral ossification.

Combination of CCN2 and BMP-2 Modulates the CCN2 or BMP-2 Signalling in Chondrocytes—Because CCN2 interacted with BMP-2 *in vitro* and co-localized with BMP-2 *in vivo*, we tested whether the combination of CCN2 and BMP-2 modulated CCN2 or BMP-2 signalling in chondrocytes, or not. As shown in Fig. 3, we performed western blot analysis of mouse costal

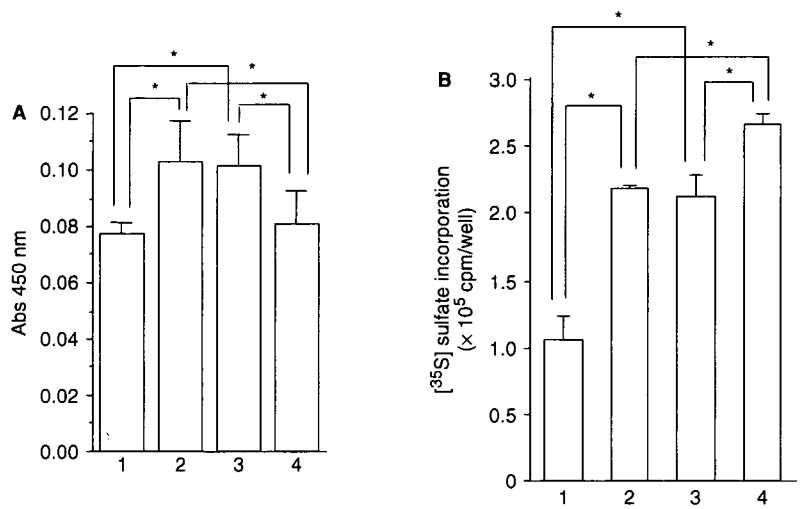

Fig. 4. **Combinational effect of CCN2 and BMP-2 on the proliferation and differentiation of HCS-2/8 cells.** (A) Effect of the combination of CCN2 and BMP-2 on the proliferation of HCS-2/8 cells. HCS-2/8 cells in DMEM containing 10% FBS were inoculated at a density of 1×10^4/well into the wells of a 96-well multiplate and cultured for 24 h. Then, the cells were stimulated with final concentrations of 50 ng/ml rBMP-2, 100 ng/ml rCCN2 or the combination of CCN2 (100 ng/ml) and BMP-2 (50 ng/ml) for 24 h. The mixture of CCN2 with BMP-2 was prepared and kept on ice for 2 h before the stimulation. The proliferation assay was performed as described in 'MATERIALS AND METHODS' section. Column 1 represents cells cultured with PBS (control); column 2, those with rBMP-2; column 3, those with rCCN2; and column 4, those with the combination of both. Asterisks indicate significant differences ($P < 0.05$) between values indicated by the brackets. Each column shows the mean value and SD of the results from 8 wells. (B) Effect of the combination of CCN2 and BMP-2 on proteoglycan synthesis in HCS-2/8 cells. Once HCS-2/8 cells had reached sub-confluence, they were treated with PBS (column 1), rBMP-2 (column 2), rCCN2 (column 3) or both (column 4) for 22 h at 37°C. At 5 h after the addition of these factors, [^{35}S]sulfate was added to the cultures; and radioactivity incorporated into proteoglycans was measured 17 h later. Values represent the means ± SD of four independent cultures. Column 1 represents cells cultured with PBS (control), column 2, those with rBMP-2; column 3, those with rCCN2; and column 4, those with both CCN2 and BMP-2. Asterisks indicate significant differences ($P < 0.05$) between values indicated by the brackets.

chondrocytes stimulated with rCCN2, rBMP-2 or their combination for 15 or 30 min by using anti-phospho-Smad1/5/8, anti-phospho-ERK1/2 and anti-phospho-p38 antibodies. The levels of Smad1/5/8 and ERK1/2 phosphorylation were increased by 50 ng/ml rBMP-2 and the phosphorylation of ERK1/2 was induced by 100 ng/ml rCCN2. However, the degree of their phosphorylation by the combination of rCCN2 and rBMP-2 was rather decreased compared with that by either factor alone (Fig. 3). Similar results were obtained in HCS-2/8 cells (data not shown). On the other hand, phospho-p38 levels were not affected by the combination of rCCN2 and rBMP-2. After 30 min of stimulation, no effect on Smad1/5/8, ERK1/2 or p38 phosphorylation was detected (data not shown). These findings suggest that the co-presence of CCN2 and BMP-2 modulates BMP-2 or CCN2 signalling in chondrocytes.

Effect of Combination of CCN2 and BMP-2 on the Proliferation and Differentiation of HCS-2/8 Cells—Because the combination of CCN2 and BMP-2 modulated CCN2 or BMP-2 signalling, we next investigated the biological significance of the combination of CCN2 and BMP-2 in HCS-2/8 cells. HCS-2/8 cells have retained the mature chondrocytic phenotype during a number of passages, and their responsiveness to growth factors and cytokines is similar to that of primary chondrocytes (*21*). Therefore, we first studied the effect of the combination of CCN2 and BMP-2 on the proliferation of the cells. As shown in Fig. 4A, rCCN2 or rBMP-2 tested alone stimulated the proliferation of the cells, but their combination showed no stimulatory effect. Second, to investigate the effect of the combination of CCN2 and BMP-2 on the differentiation of HCS-2/8 cells, we evaluated proteoglycan synthesis, which is a good marker of differentiated chondrocytes, in the cells stimulated by the combination of rCCN2 and rBMP-2. As shown in Fig. 4B, either rBMP-2 or rCCN2 alone stimulated the proteoglycan synthesis, which was consistent with previous studies (*13*, *14*, *25*). Interestingly, when the combination of CCN2 and BMP-2 was added to the culture of HCS-2/8 cells, proteoglycan synthesis was additively increased. These findings suggest that the combination of CCN2 and BMP-2 collaboratively promoted the differentiation of HCS-2/8 cells but that the proliferation was rather interfered with by the combination.

Effect of Combination of CCN2 and BMP-2 on the Expression of Chondrocyte Marker Genes and Differentiation of Mouse Primary Chondrocytes—To clarify in detail the differentiation of chondrocytes stimulated with the combination of CCN2 and BMP-2, we performed northern blot analysis of various cartilage differentiation markers, i.e. type II collagen, aggrecan, type X collagen and Runx2/Cbfa1. As shown in Fig. 5A,

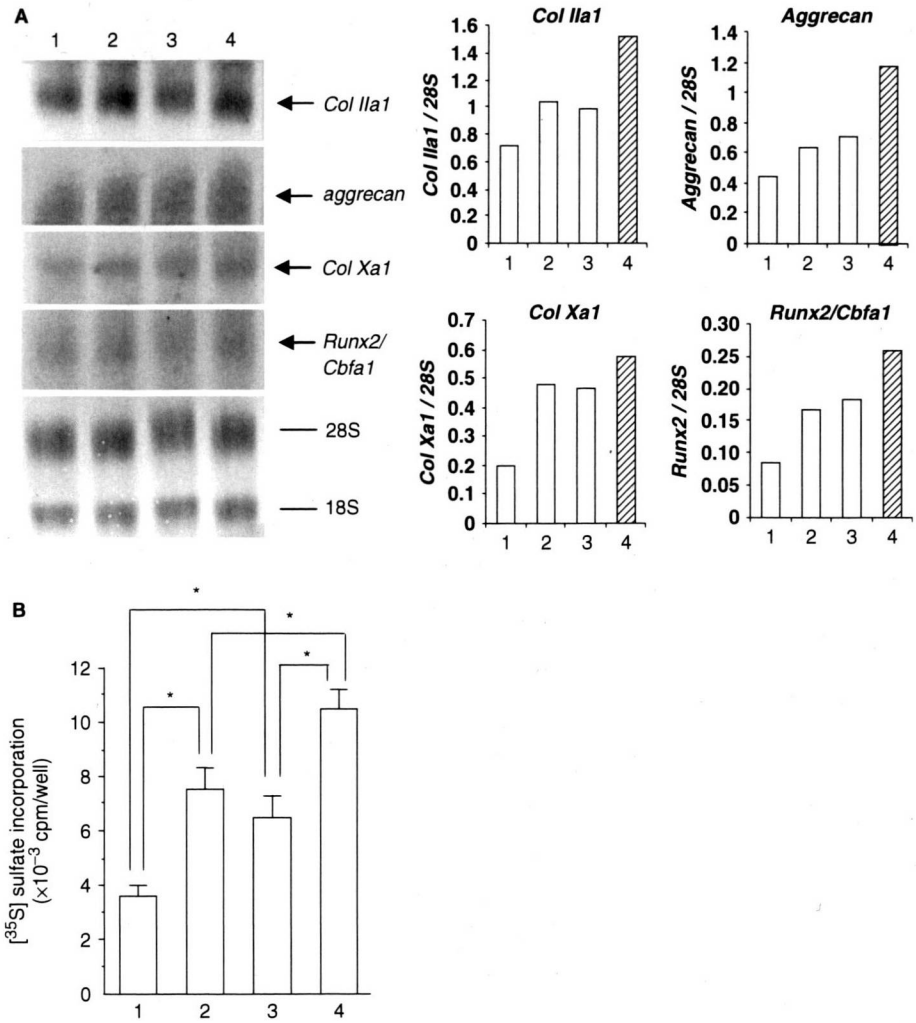

Fig. 5. **Combinational effect of CCN2 and BMP-2 on expression of the differentiated phenotype of chondrocytes in mouse chondrocytes in culture.** (A) Northern blot analysis of the expression of type II collagen, aggrecan, type X collagen and Runx2/Cbfa1 in mouse chondrocytes. Mouse primary chondrocytes were re-plated into 6 cm dishes, and they were then cultured until they had reached confluence. Thereafter, the medium was replaced with serum-free medium containing rBMP-2 (50 ng/ml), rCCN2 (100 ng/ml) or the combination of CCN2 and BMP-2; and total RNA was prepared 6 h later. Northern blot analysis was performed as described in 'MATERIALS AND METHODS section'. Hybridization signals of cartilage marker genes in the autoradiogram and methylene blue-stained rRNA on the same membrane are displayed. Representative results of treatment with PBS (lane 1), rBMP-2 (lane 2), rCCN2 (lane 3) and their combination (lane 4) are shown. The amounts of cartilage marker genes were normalized to the amounts of 28S rRNA. (B) Effect of the combination of CCN2 and BMP-2 on proteoglycan synthesis in mouse chondrocytes. After mouse chondrocytes of passage 1 had reached subconfluence, the medium was replaced with αMEM containing 0.5% FBS and PBS (lane 1), rBMP-2 (50 ng/ml, lane 2), rCCN2 (100 ng/ml, lane 3) or the combination of CCN2 and BMP-2 (lane 4); and incubation was further continued for 22 h at 37°C. After 5 h of stimulation, [^{35}S]sulfate was added to the cultures; and radioactivity incorporated into proteoglycans was then measured. Values represent means ± SD of four cultures. Asterisks indicate significant differences ($P < 0.05$) between values indicated by the brackets.

the expression of type II collagen and aggrecan, which are good markers of mature chondrocytes, was promoted by the combination of rCCN2 and rBMP-2 better than that by each factor alone. In addition, the combination of rCCN2 and rBMP-2 also stimulated the expression of type X collagen and Runx2/Cbfa1, which are markers of hypertrophic chondrocytes, to a greater degree than each factor alone. Furthermore, to confirm whether or not combination of CCN2 and BMP-2 stimulated proteoglycan synthesis in a synergistic or additive manner, we treated mouse costal chondrocyte cultures with the combination of rCCN2 and rBMP-2 (Fig. 5B). As shown in Fig. 5B, the combination of rCCN2 and rBMP-2 increased proteoglycan synthesis additively, consistent with the result in Fig. 4B. These results suggest that the combination of CCN2 and BMP-2 stimulates chondrocyte differentiation better than CCN2 or BMP-2 alone.

DISCUSSION

In this study, we demonstrated that CCN2 directly interacted with BMP-2. It was previously reported that CCN2 directly bound BMP-4 through its VWC domain and that CCN2 inhibited BMP-4 action (*10*). The same study also showed, by western blot analysis, that the binding of BMP-4 to CCN2 could be competed by an excess of BMP-2, which suggests that CCN2 also binds to BMP-2 through the same domain (*10*). This VWC domain is 80% homologous to chordin, which is a BMP antagonist in terms of the cysteine residues (*26*). Therefore, this finding indicates that CCN2 may be a novel BMP antagonist. In this study, we investigated whether CCN2 directly binds to BMP-2 and functions as a BMP-2 antagonist, or not. BMP-2 has various effects on cartilage metabolism (*13*, *14*). It was reported that BMP-2 stimulated the proliferation, maturation and hypertrophy of chondrocytes *in vitro* (*13*, *14*), but apparently contradictory results were obtained in an *in vivo* study using genetically modified mice (*15–18*). These findings suggest that there are many factors regulating BMP signalling *in vivo*. In the solid-phase binding assay using each recombinant module protein, we showed that CCN2 bound to BMP-2 mainly through its CT module and partially through its IGFBP and VWC modules (Fig. 1C). In addition, we confirmed that binding of TSP1-CT fragment to BMP-2 was more prominent than that of IGFBP-VWC fragment (Fig. 1D). Inkson *et al.* reported that [CXXXCXC] and [CCXXC] motifs, which are typical chordin cysteine-rich (CR) sequences, have been conserved in the VWC domain of CCN2 binding to BMPs (*26*). It should be noted that reversed [CXCXXXC] and [CXXCC] motifs are present in the CT module of CCN2. Therefore, BMP-2 may bind to CCN2 probably via these sequences in the CT module as well.

The crystal structure of CCN2 is still unknown. Previously, we raised several monoclonal antibodies against CCN2 by using a recombinant full-length CCN2 protein as an immunogen, and located the epitopes in the module in CCN2. As a result, we found that two of five monoclonal antibodies recognized the VWC module (*27*). These results indicate the strong antigenicity of the VWC module and suggest that this module is exposed on the molecular surface. In addition, it has been suggested that CCN2 forms a dimer *via* the CT domain (*28*), and that CT domain also directly interacts with ECM proteins, such as fibronectin and heparan sulfate (*28*, *29*). Under the condition that CCN2 is overexpressed in the cells, the binding of BMP-2 to the CT domain may not occur, because this domain is engaged in the dimerization of CCN2 or interacts with ECM. Thus, the VWC module may be more accessible than the CT module. If so, the VWC module may be a major interface for CCN2-BMP interaction. Nevertheless, we showed the binding of CT module to BMP-2 and the modest binding of IGFBP and VWC modules in this binding study; hence, binding of VWC module to BMP-2 may require the collaboration of the IGFBP module to confer the full binding activity. In fact, we showed that the amount of total binding of TSP1-CT and IGFBP-VWC fragments to BMP-2 was comparable with the binding of full-length CCN2. These findings suggest that both IGFBP-VWC and CT domains contribute to the interaction of CCN2 with BMP-2.

BMPs transduce signals by binding to heteromeric complexes of type I and type II serine/threonine kinase receptors. The binding of BMPs to the receptor complex results in the phosphorylation of intracellular Smads, which then are translocated to the nucleus, where they regulate the transcription of the target genes (*5*, *16*, *30*). On the other hand, it has been also reported that BMPs transduce signals by the activation of mitogen-activated protein kinase (MAPK) pathways (*5*, *30*) and that the activation of MAPK, especially the p38 pathway, plays an important role in chondrocyte differentiation (*31*). In addition, the expression of the Runx2/Cbfa1 gene, which induces cartilage hypertrophy, is up-regulated by rBMP-2 treatment (*30*, *32*). In this study, we showed that phosphorylation of Smad1/5/8 induced by BMP-2 treatment was inhibited by the co-presence of CCN2. Furthermore, the activation of ERK1/2 and p38 MAPK pathways was induced by BMP-2, but phosphorylation of ERK1/2 was dramatically decreased by the co-presence of CCN2 with BMP-2 in chondrocytes (Fig. 3). These results suggest that CCN2 binds to BMP-2 and regulates the BMP signalling pathways. Typical antagonists, such as noggin, chordin and follistatin, bind to BMPs and prevent them from interacting with their receptors (*30*, *33*). The major difference between CCN2 and other BMP antagonists is that CCN2 itself is a growth factor and activates the signalling to the nucleus. We reported that the phosphorylation of ERK1/2 was involved in chondrocyte proliferation and that the phosphorylation of p38 MAPK was involved in chondrocyte differentiation induced by rCCN2 (*34*). In fact, we showed presently that the co-presence of CCN2 with BMP-2 inhibited chondrocyte proliferation and promoted proteoglycan synthesis in HCS-2/8 cells (Fig. 4). In addition, this co-presence increased the gene expression of chondrocyte differentiation markers, such as type II collagen, aggrecan and type X collagen, and promoted proteoglycan synthesis in mouse chondrocytes as well as in HCS-2/8 cells (Fig. 5). Also, we reported that PD98059, which is a specific MEK inhibitor, blocked chondrocyte proliferation and stimulated proteoglycan synthesis in HCS-2/8 cells (*34*). Considering these findings, a decrease in ERK1/2 signalling caused by the complex formation of CCN2 with BMP-2 may lead to the inhibition of the proliferation and promotion of the differentiation of chondrocytes. The expression of type X collagen mRNA, which is a marker of chondrocyte hypertrophy, was also increased by the combination of CCN2 and BMP-2 treatment, in spite of the decreased Smad1/5/8 phosphorylation representing the classical BMP signalling. However, we also showed that the gene expression of Runx2/Cbfa1 was increased by the combination of CCN2 and BMP-2 treatment of chondrocytes (Fig. 5). Therefore, we propose that the level of expression of type X collagen mRNA was increased due to the up-regulation of Runx2/Cbfa1 induced by stimulation from the combination of CCN2 and BMP-2. Taken together, these findings indicate that CCN2 interacted with BMP-2 to inhibit chondrocyte proliferation and to promote differentiation, thus suggesting that CCN2 modulates not only BMP signalling but also its own signalling to regulate the chondrocyte

proliferation and differentiation as a 'signal conductor'. We conclude that CCN2 has both antagonistic effect and agonistic effect of BMP-2 during endochondral ossification.

FUNDING

This work was supported in part by the programs Grants-in-Aid for Medical and Dental Postgraduate Education (to A.M.) and Exploratory Research (to M.T.) of the Ministry of Education, Culture, Sports, Science, and Technology, Japan, and Grants-in-Aid for Scientific Research (S) (to M.T.) and (C) (to S.K.) from Japan Society for the Promotion of Sciences.

ACKNOWLEDGEMENT

We thank Drs Takako Hattori and Harumi Kawaki for their helpful suggestions and are also grateful to Yoko Tada for secretarial assistance.

CONFLICT OF INTEREST

None declared.

REFERENCES

1. Zelzer, E. and Olsen, B.R. (2003) The genetic basis for skeletal diseases. *Nature* **423**, 343–348
2. Shimizu, H., Yokoyama, S., and Asahara, H. (2007) Growth and differentiation of the developing limb bud from the perspective of chondrogenesis. *Develop. Growth Differ.* **49**, 449–454
3. Redini, F., Galera, P., Mauviel, A., Loyau, G., and Pujol, J.P. (1988) Transforming growth factor β stimulates collagen and glycosaminoglycan biosynthesis in cultured rabbit articular chondrocytes. *FEBS Lett.* **234**, 172–176
4. Trippel, S.B. (1992) Role of insulin-like growth factors in the regulation of chondrocytes *in Biological Regulation of the Chondrocytes* (Adolphe, M., ed.) pp. 161–190, CRC Press, Boca Raton, FL
5. Yoon, B.S. and Lyons, K.M. (2004) Multiple functions of BMPs in chondrogenesis. *J. Cell. Biochem.* **93**, 93–103
6. Kubota, S. and Takigawa, M. (2007) Role of CCN2/CTGF/Hcs24 in bone growth. *Int. Rev. Cytol.* **257**, 1–41
7. Nakanishi, T., Nishida, T., Shimo, T., Kobayashi, K., Kubo, T., Tamatani, T., Tezuka, K., and Takigawa, M. (2000) Effects of CTGF/Hcs24, a product of a hypertrophic chondrocyte-specific gene, on the proliferation and differentiation of chondrocytes in culture. *Endocrinology* **141**, 264–273
8. Nishida, T., Kubota, S., Kojima, S., Kuboki, T., Nakao, K., Kushibiki, T., Tabata, Y., and Takigawa, M. (2004) Regeneration of defects in articular cartilage in rat knee joints by CCN2 (connective tissue growth factor). *J. Bone Miner. Res.* **19**, 1308–1319
9. Ivkovic, S., Yoon, B.S., Popoff, S.N., Safadi, F.F., Libuda, D.E., Stephenson, R.C., Daluiski, A., and Lyons, K.M. (2003) Connective tissue growth factor coordinates chondrogenesis and angiogenesis during skeletal development. *Development* **130**, 2779–2791
10. Abreu, J.G., Ketpura, N.I., Reversade, B., and de Robertis, E.M. (2002) Connective-tissue growth factor (CTGF) modulates cell signalling by BMP and TGF-β. *Nat. Cell Biol.* **4**, 599–604
11. Inoki, I., Shiomi, T., Hashimoto, G., Enomoto, H., Nakamura, H., Makino, K., Ikeda, E., Takata, S., Kobayashi, K., and Okada, Y. (2002) Connective tissue growth factor binds vascular endothelial growth factor (VEGF) and inhibits VEGF-induced angiogenesis. *FASEB J.* **16**, 219–221
12. Wozney, J.M. (1989) Bone morphogenetic proteins. *Prog. Growth Factor Res.* **1**, 267–280
13. Valcourt, U., Ronzière, M.-C., Winkler, P., Rosen, V., Herbage, D., and Mallein-Gerin, F. (1999) Different effects of bone morphogenetic proteins 2, 4, 12, and 13 on the expression of cartilage and bone markers in the MC615 chondrocyte cell line. *Exp. Cell Res.* **251**, 264–274
14. Shukunami, C., Ohta, Y., Sakuda, M., and Hiraki, Y. (1998) Sequential progression of the differentiation program by bone morphogenetic protein-2 in chondrogenic cell line ATDC5. *Exp. Cell Res.* **241**, 1–11
15. Tsuji, K., Bandyopadhyay, A., Harfe, B.D., Cox, K., Kakar, S., Gerstenfeld, L., Einhorn, T., Tabin, C.J., and Rosen, V. (2006) BMP2 activity, although dispensable for bone formation, is required for the initiation of fracture healing. *Nat. Genet.* **38**, 1424–1429
16. von Bubnoff, A. and Cho, K.W. (2001) Intracellular BMP signaling regulation in vertebrates: pathway or network? *Dev. Biol.* **239**, 1–14
17. Tsuji, K., Cox, K., Bandyopadhyay, A., Harfe, B.D., Tabin, C.J., and Rosen, V. (2008) BMP4 is dispensable for skeletogenesis and fracture-healing in the limb. *J. Bone Joint Surg. Am.* **90**, 14–18
18. Bandyopadhyay, A., Tsuji, K., Cox, K., Harfe, B.D, Rosen, V., and Tabin, C.J. (2006) Genetic analysis of the roles of BMP2, BMP4, and BMP7 in limb patterning and skeletogenesis. *PLoS Genet.* **2**, 2116–2130
19. Yoon, B.S., Ovchinnikov, D.A., Yoshii, I., Mishina, Y., Behringer, R.R., and Lyons, K.M. (2005) Bmpr1a and Bmpr1b have overlapping functions and are essential for chondrogenesis in vivo. *Proc. Natl. Acad. Sci. USA.* **102**, 5062–5067
20. Nishida, T., Nakanishi, T., Shimo, T., Asano, M., Hattori, T., Tamatani, T., Tezuka, K., and Takigawa, M. (1998) Demonstration of receptors specific for connective tissue growth factor on a human chondrocytic cell line (HCS-2/8). *Biochem. Biophys. Res. Commun.* **247**, 905–909
21. Takigawa, M., Tajima, K., Pan, H.-O., Enomoto, M., Kinoshita, A., Suzuki, F., Takano, Y., and Mori, Y. (1989) Establishment of a clonal human chondrosarcoma cell line with cartilage phenotypes. *Cancer Res.* **49**, 3996–4002
22. Nishida, T., Kawaki, H., Baxter, R.M., Deyoung, R.A., Takigawa, M., and Lyons, K.M. (2007) CCN2 (connective tissue growth factor) is essential for extracellular matrix production and integrin signaling in chondrocytes. *J. Cell Commun. Signal.* **1**, 45–58
23. Nishida, T., Kubota, S., Fukunaga, T., Kondo, S., Yosimichi, G., Nakanishi, T., Takano-Yamamoto, T., and Takigawa, M. (2003) CTGF/Hcs24, hypertrophic chondrocyte-specific gene product, interacts with perlecan in regulating the proliferation and differentiation of chondrocytes. *J. Cell. Physiol.* **196**, 265–275
24. Yamaai, T., Nakanishi, T., Asano, M., Nawachi, K., Yosimichi, G., Ohyama, K., Komori, T., Sugimoto, T., and Takigawa, M. (2005) Gene expression of connective tissue growth factor (CTGF/CCN2) in calcifying tissues of normal and *cbfa1*-null mutant mice in late stage of embryonic development. *J. Bone Miner. Metab.* **23**, 280–288
25. Nishida, T., Kubota, S., Nakanishi, T., Kuboki, T., Yosimichi, G., Kondo, S., and Takigawa, M. (2002) CTGF/Hcs24, a hypertrophic chondrocyte-specific gene product, stimulates proliferation and differentiation, but not hypertrophy of cultured articular chondrocytes. *J. Cell. Physiol.* **192**, 55–63
26. Inkson, C.A., Ono, M., Kuznetsov, S.A., Fisher, L.W., Gehron Robey, P., and Young, M.F. (2008) TGF-β1 and WISP-1/CCN4 can regulate each other's activity to cooperatively control osteoblast function. *J. Cell. Biochem.* **104**, 1865–1878

27. Minato, M., Kubota, S., Kawaki, H., Nishida, T., Miyauchi, A., Hanagata, H., Nakanishi, T., Takano-Yamamoto, T., and Takigawa, M. (2004) Module-specific antibodies against human connective tissue growth factor: utility for structural and functional analysis of the factor as related to chondrocytes. *J. Biochem.* **135**, 347–354
28. Brigstock, D.R., Steffen, C.L., Kim, G.Y., Vegunta, R.K., Diehl, J.R., and Harding, P.A. (1997) Purification and characterization of novel heparin-binding growth factors in uterine secretory fluids: identification as heparin-regulated Mr 10,000 forms of connective tissue growth factor. *J. Biol. Chem.* **272**, 20275–20282
29. Hoshijima, M., Hattori, T., Inoue, M., Araki, D., Hanagata, H., Miyauchi, A., and Takigawa, M. (2006) CT domain of CCN2/CTGF directly interacts with fibronectin and enhances cell adhesion of chondrocytes through integrin α5β1. *FEBS Lett.* **580**, 1376–1382
30. Tsumaki, N. and Yoshikawa, H. (2005) The role of bone morphogenetic proteins in endochondral bone formation. *Cytokine Growth Factor Rev.* **16**, 279–285
31. Stanton, L.-A., Underhill, T. M., and Beier, F. (2003) MAP kinases in chondrocyte differentiation. *Dev. Biol.* **263**, 165–175
32. de Crombrugghe, B., Lefebvre, V., and Nakashima, K. (2001) Regulatory mechanisms in the pathways of cartilage and bone formation. *Curr. Opin. Cell Biol.* **13**, 721–727
33. Balemans, W. and Vau Hul, W. (2002) Extracellular regulation of BMP signaling in vertebrates: a cocktail of modulators. *Dev. Biol.* **250**, 231–250
34. Yosimichi, G., Kubota, S., Nishida, T., Kondo, S., Yanagita, T., Nakao, K., Takano-Yamamoto, T., and Takigawa, M. (2006) Roles of PKC, PI3K and JNK in multiple transduction of CCN2/CTGF signals in chondrocytes. *Bone* **38**, 853–863

JBC Papers in Press. Published on April 19, 2010 as Manuscript M110.127027
The latest version is at http://www.jbc.org/cgi/doi/10.1074/jbc.M110.127027

PANNEXIN 3 REGULATES INTRACELLULAR ATP/cAMP LEVELS AND PROMOTES CHONDROCYTE DIFFERENTIATION

Tsutomu Iwamoto[1,2], Takashi Nakamura[1,2], Andrew Doyle[1], Masaki Ishikawa[1], Susana de Vega[1], Satoshi Fukumoto[2], and Yoshihiko Yamada[1]

[1]Laboratory of Cell and Developmental Biology, National Institute of Dental and Craniofacial Research, National Institutes of Health, Bethesda, Maryland 20892-4370, USA; [2]Department of Pediatric Dentistry, Tohoku University Graduate School of Dentistry, Sendai 980-8576, Japan

Running head: Pannexin 3 and chondrocyte differentiation
Address correspondence to: Yoshihiko Yamada, PhD. Bldg. 30, Rm. 407, NIDCR, NIH, 30 Convent Drive MSC 4370, Bethesda, MD 20892-4370. Tel: 301-496-2111; Fax: 301-402-0897; E-mail: yoshi.yamada@nih.gov

Pannexin 3 (Panx3) is a new member of the gap junction pannexin family, but its expression profiles and physiological function are not yet clear. We demonstrate in this paper that Panx3 is expressed in cartilage and regulates chondrocyte proliferation and differentiation. *Panx3* mRNA was expressed in the prehypertrophic zone in the developing growth plate and was induced during the differentiation of chondrogenic ATDC5 and N1511 cells. Panx3-transfected ATDC5 and N1511 cells promoted chondrogenic differentiation, but the suppression of endogenous Panx3 inhibited differentiation of ATDC5 cells and primary chondrocytes. Panx3-transfected ATDC5 cells reduced PTH-induced cell proliferation and promoted the release of ATP into the extracellular space, possibly by action of Panx3 as a hemichannel. Panx3 expression in ATDC5 cells reduced intracellular cAMP levels and the activation of CREB, a PKA downstream effector. These Panx3 activities were blocked by anti-Panx3 antibody. Our results suggest that Panx3 functions to switch the chondrocyte cell fate from proliferation to differentiation by regulating the intracellular ATP/cAMP levels.

Cartilage plays an important role in mechanical load resistance and in skeletal structure support. It also serves as the skeletal template for endochondrial ossification by which most bones in the body, such as long bones, are formed. In endochondral ossification, cartilage development is initiated by mesenchymal cell condensation, followed by a series of proliferation and differentiation processes. Cells undergoing condensation differentiate into chondrocytes, which then proliferate, produce type II collagen, and form the proliferative zone of the cartilage molds. As development proceeds, chondrocytes in the center of the cartilage molds (prehypertrophic zone) cease proliferating and differentiate into type X collagen-producing hypertrophic chondrocytes, to form the hypertrophic zone. Terminally differentiated hypertrophic chondrocytes mineralize the surrounding matrix. Eventually these cells die by apoptosis and are replaced by osteoblasts that form trabecular bone.

The regulation of chondrocyte proliferation and differentiation must be tightly coordinated, in order to allow formation of properly sized cartilage and bone (1). Parathyroid-hormone-related peptide (PTHrP) and parathyroid hormone (PTH) sustain chondrocyte proliferation and delay differentiation of the growth plate (2). PTHrP is expressed by perichondrial cells and chondrocytes in the upper region of growing cartilage. Mutant mice that are deficient in PTHrP (3), PTH (4), or its receptor (5) have short proliferative zones and accelerated chondrocyte differentiation, which results in abnormal endochondrial bone formation. In contrast, mice that overexpress PTHrP have enlarged proliferative zones and delayed chondrocyte terminal differentiation (6). Humans with an activating mutation in the PTH/PTHrP receptor develop Jansen's metaphyseal chondrodysplasia, characterized by

disorganization of the growth plates and delayed chondrocyte terminal differentiation (7). These results suggest that PTH/PTHrP signaling regulates skeletal development by promoting cell proliferation and inhibiting hypertrophic differentiation of chondrocytes.

The binding of PTH/PTHrP to its receptor activates both G_s and G_q family heterotrimeric G proteins (8,9). The activation of G_s is necessary for cAMP production and protein kinase A (PKA) activation, which leads to phosphorylation of the cAMP response element binding (CREB) family of transcription factors. CREB then induces genes such as the cyclin D1 and cyclin A genes. The activated cyclin/cyclin-dependent kinases in turn phosphorylate the retinoblastoma protein (pRB) and its relative factors, which then dissociates the E2F transcription factor and subsequently activates the target genes necessary for DNA replication and cell cycle progression. Thus CREB is a direct target of PKA and a downstream target of PTH/PTHrP/cAMP signaling and is required for chondrocyte proliferation (10,11). How proliferation signaling is downregulated in the prehypertrophic zone to stop proliferation and allow the switch to the postmitotic state, is not well understood.

Pannexins, relatives of innexins that had been considered as exclusively invertebrate gap junction proteins, were recently discovered as candidates for a second family of gap junction proteins in vertebrates (12). Although there are some similarities in domain structures between pannexins and connexins, which are well characterized as vertebrate gap junction proteins, these 2 protein families have no sequence homology (13). The pannexin family has 3 members: pannexin 1 (Panx1), pannexin 2 (Panx2), and pannexin 3 (Panx3). These proteins were originally identified in the human and mouse genomes (12). The expression of Panx1 is observed in many organs, such as the eye, thyroid, prostate, kidney, and liver, but its expression is especially strong in both the developing and mature central nervous system (CNS) (12-14). Panx2 is preferentially expressed in the CNS. Recently, it was reported that Panx3 is expressed in skin, cartilage, and cochlea (15-17).

In *Xenopus* oocytes, Panx1 forms both non-junctional hemichannels and intercellular channels and interacts with Panx2 (18). Panx1 hemichannels are stress-sensitive conduits for ATP (19). Panx1 is a Ca^{2+}-permeable ion channel that is localized on both the ER and plasma membrane, and participates in ER Ca^{2+} leakage and intercellular Ca^{2+} movement (20). Both Panx1 and Panx3 are glycoproteins and N-glycosylation of these pannexins plays a role in intracellular trafficking and functional channel function (15,16). The physiological function of pannexins in cell differentiation has not yet been characterized, however.

In this paper, we report that Panx3 regulates the proliferation and differentiation of chondrocytes. *Panx3* mRNA was expressed in prehypertrophic chondrocytes and induced during the differentiation of chondrogenic ATDC5 cells. The transfection of Panx3 into ATDC5 cells promoted ATDC5 cell differentiation, whereas the inhibition of endogenous Panx3 by shRNA blocked differentiation. Panx3 promoted ATP release into the extracellular space and inhibited PTH-mediated cell proliferation, intracellular levels of cAMP, and phosphorylation of CREB. Thus our results suggest that Panx3 regulates the transition of proliferation to differentiation in chondrocytes.

EXPERIMENTAL PROCEDURES

Reagents— Insulin-transferrin-sodium selenite (ITS) was obtained from Sigma. Recombinant rat PTH (1-34) was purchased from Bachem. Recombinant human BMP2 was purchased from Humanzyme.

In situ hybridization— Digoxigenin-11-UTP-labeled, single-stranded antisense RNA probes for *Panx3*, *Ihh*, *Col2a1*, *Col10a1*, and *Hist1h4c* were prepared using the DIG RNA labeling kit (Roche Applied Science) according to the manufacturer's instructions. In situ hybridization of the tissue sections was performed essentially according to the protocol provided with Link-Label ISH Core Kit (Biogenex). Frozen tissue sections from growth plates (E16.5) were generated and placed on RNase-free glass slides. After

drying the frozen sections for 10 min at room temperature and incubating at 37°C for 30 min, the sections were treated with 10 μg/ml of proteinase K at 37°C for 30 min. Hybridization was performed at 37°C for 16 h, and washes were carried out with 2x SSC at 50°C for 15 min and 2x SSC containing 50% formamide at 37°C for 15 min. The slides were then subjected to digestion with 10 μg/ml RNase A in 10 mM Tris-HCl (pH 7.6), 500 mM NaCl, and 1 mM EDTA at 37°C for 15 min and then washed. The sections were treated with 2.4 mg/ml Levamisol (Sigma) to inactivate endogenous alkaline phosphatase.

Antibody for Panx3— A rabbit polyclonal antibody to a peptide (amino acid residues, HHTQDKAGQYKVKSLWPH) from the first extracellular loop of the mouse Panx3 protein was prepared. The antiserum was purified by the peptide affinity column. This purified antibody reacts specifically to Panx3 and was used for immunohistochemistry, Western blotting, and functional blocking assay. For inhibition by the Panx3-antibody, the cells were incubated with 10 ng/ml affinity-purified antibody or control IgG for 30 min before the experiments. To abrogate the blocking activity with Panx3-antibody, the Panx3 peptide was pre-incubated with the Panx3-antibody. A peptide with a scrambled sequence (WHTKYQVGLDPQHKASHK) of the Panx3 peptide was used as a control.

Immunohistochemistry— Frozen tissue sections were fixed with acetone at -20°C for 2 min and treated with L.A.B. (Liberate Antibody Binding) solution for 15 min at 37°C. For cultured cell staining, the cells were fixed with acetone at -20°C for 2 min. Immunohistochemistry was performed on sections that were incubated with Universal Blocking Reagent (BioGenex) for 7 min at room temperature before incubation with the primary antibody. The primary antibodies were detected by Cy-3- or Cy-5-conjugated secondary antibodies (Jackson ImmunoResearch Laboratories). Nuclear staining was performed with Hoechst dye (Sigma-Aldrich). A fluorescence microscope (Axiovert 200; Carl Zeiss MicroImaging, Inc.) and 510 Meta Confocal Microscope (Zeiss) were used for immunofluorescent image analysis. For GFP and ER-Tracker Red (Invitrogen) staining, ATDC5 cells were transfected for 2 days and then stained with ER-Tracker Red as described in the manufacturer's instructions. The images were prepared with AxioVision and Photoshop (Adobe Systems, Inc.).

Cell culture— ATDC5 cells (21) were grown in Dulbecco's modified Eagle's medium/F-12 (Life Technologies, Inc.) containing 5% fetal bovine serum (HyClone) and under 5% CO_2. In proliferation conditions, cells were maintained under confluency, and the media were replaced every other day. In differentiation conditions, cells were plated in confluency and incubated in the same medium plus 10 μg/ml of insulin, 10 μg/ml of transferrin, and 10 μg of selenium. N1511 cells (22) were cultured with α-MEM (Life Technologies, Inc.) containing 2% fetal bovine serum (HyClone) under 5% CO_2. As differentiation conditions, 1 μM insulin, 100 ng/ml rhBMP2, and 50 μg/ml ascorbic acid were added in the culture medium.

Mouse primary chondrocytes were isolated from neonatal ICR mice as previously described (23). Distal cartilaginous ends of femurs and humeri were digested with 0.25% trypsin/0.01% EDTA for 15 min, followed by digestion with 2 mg/ml collagenase type I (Worthington) in DMEM/F-12 overnight. Neonatal mouse cartilage tissue was dispersed by pipetting, and cells were filtered through 100 μm cell strainers (FALCON). Single cells were inoculated onto type I collagen-coated multiwell dishes maintained in 10% FBS in αMEM.

RT-PCR and real-time PCR— Total RNA was extracted from cells using the Trizol reagent kit (Invitrogen). Two μg of total RNA was used for reverse transcription to generate cDNA, which was used as a template for PCR with gene-specific primers. Each cDNA was amplified with an initial denaturation at 95°C for 3 min; then 95°C for 30 s, 60°C for 30 s, and 72°C for 30 s for 25 cycles; and a final elongation step at 72°C for 5 min and then separated on agarose gels. Real-time PCR was performed

with SYBR Green PCR Master Mix and the TaqMan 7700 Sequencer Detection System (Applied Biosystems). PCR was performed for 40 cycles, 95°C for 1 min, 60°C for 1 min, and 72°C for 1 min. Gene expression was normalized to the housekeeping gene *S29*. The reactions were run in triplicate and repeated 3 times, and the results were combined to generate the graphs. The following primer sequences were used: *Panx3*, 5'-GCCCCTGGATAAGATGGTCAAG -3' and 5'- GCGGATGGAACGGTTGTAAGA -3'; *Panx1*, 5'-TTTGGACCTAAGAGACGGACCTG -3' and 5'-CGGGAATCAGCAGAGCATACAC -3'; *Panx2*, 5'-ACAAGGGCAGTGGAGGTGATTC -3' and 5'-CGATGAGGATAGCGTGCTGATG -3'; *Col2a1*, 5'-GAAAAACTGGTGGAGCAGCAAGAGC -3' and 5'-CAATAATGGGAAGGCGGGAGGTC -3'; *Agc1*, 5'-TGGAGCATGCTAGAACCCTCG -3' and 5'- GCGACAAGAAGACACCATGTG -3'; *Col10a1*, 5'-AGCCCCAAGACACAATACTTCATC -3' and 5'-TTTCCCCTTTCCGCCCATTCACAC -3'; *PPR*, 5'-ACTACTACTGGATTCTGGTGGAGGG -3' and 5'-CTGGAAGGAGTTGAAGAGCATCTC -3'; *PTHrP*, 5'-CAGACGATGAGGGCAGATACCTAAC -3' and 5'-CAGTTTCCTGGGGAGACAGTTTG -3'; and *Gapdh*, 5'-ACCACAGTCCATGCCATCAC -3' and 5'- TCCACCACCCTGTTGCTGTA -3'. The predicted size of each fragment is 373, 380, 442, 392, 325, 463, 470, 558, 470, 372, and 452 base pairs, respectively.

Western blotting— The cells were washed 3 times with phosphate-buffered saline containing 1 mM sodium vanadate (Na_3VO_4), then solubilized in 100 µl of lysis buffer (10 mM Tris-HCl (pH 7.4), 150 mM NaCl, 10 mM $MgCl_2$, 0.5% Nonidet P-40, 1 mM phenylmethylsulfonyl fluoride, and 20 units/ml aprotinin). Lysed cells were centrifuged at 14,000 rpm for 30 min, and the protein concentration of each sample was measured with Micro-BCA Assay Reagent (Pierce Chemical Co.). The samples were denatured in SDS sample buffer and loaded onto a 12% SDS-polyacrylamide gel. Ten µg of lysate protein was applied to each lane. After SDS-polyacrylamide gel electrophoresis, the proteins were transferred onto a polyvinylidene difluoride membrane and immunoblotted with anti-CREB, anti-phospho-CREB (Cell Signaling Technology, Inc.), anti-MAP kinase, and anti-phospho-MAP kinase (New England Biolabs) and then visualized using an ECL kit (Amersham Pharmacia Biotech). For CREB and ERK1/2 experiments, the cells were pretreated as follows: The cells ($3x10^4$ cell/cm^2) were plated in a 60 mm-dish and cultured with 10 µg/ml of insulin, 10 µg/ml of transferrin, and 10 µg of selenium for 7 days. They were incubated with serum-free 0.1% albumin-containing DMEM/F-12 medium for 8–12 h and then exposed to 100 nM rPTH (1-34) for the appropriate times.

Plasmid construction and transfection— The coding sequence of mouse Panx3 cDNA was subcloned into the pEF1/V5-His vector (pEF1/Panx3) and pcDNA3.1-GFP-TOPO (Panx3-pcDNA-GFP) (Invitrogen). As a control, an empty vector of pEF1 or was pcDNA3.1-GFP-TOPO used. ATDC5 cells or N1511 cells were transiently transfected using Nucleofector (Amaxa). Briefly, cells were resuspended in 100 µl of Nucleofector solution T and transfected with 5 µg of DNA using Program T-20. Transfection efficiency using these conditions was shown to be >70%. For stable transfection of ATDC5 cells, selection was initiated 24 h after transfection using G418 (Invitrogen) at a concentration of 600 µg/ml for 2 weeks. Pools of transfected cells were collected and cultured as the parental ATDC5 cells, in the continued presence of 60 µg/ml of G418. All experiments were performed 3 times, and representative experiments are shown. For transient transfection, Panx3-pcDNA-GFP was transfected into ATDC5 cells under the same conditions as used for stable transfection, except that G418 was omitted.

Alcian blue staining— The cells were first rinsed with PBS 3 times, and then fixed with 100% methanol for 10 min at –20°C. Staining was accomplished by applying a solution of 0.1% Alcian Blue 8 GX in 0.1 M HCl to the cells for 2 h at room temperature. To quantify the intensity of the staining, the stained culture plates were rinsed with PBS 3 times and the well extracted with 6 M guanidine/HCl for 8 h at room temperature. The optical density of the extracted dye was measured at 650 nm.

Short-hairpin RNA experiments— Panx3-specific knockdowns were performed with the expression of short-hairpin RNA (shRNA) using a pSM2 vector (Open Biosystems). The shRNA construct contains the 3'-untranslated region of *Panx3* (GGCAGGGTAGAACAATTTA). A non-silencing shRNA construct from Open Biosystems, whose sequence has been verified to contain no homology to known mammalian genes, was used as a control. The cells were transfected with shRNA plasmids using Nucleofection (Amaxa). Selection was performed 24 h after transfection with puromycin at a concentration of 4 μg/ml for 5 days.

siRNA experiments— siRNAs targeting mouse Panx3 (NM_172454) (Panx3 siRNA-1, 5'-UAAUAAGGAUGUCCACGUA-3' and Panx3 siRNA-2, 5'-GGGCUCAGAUUAUGGACUA-3') were purchased from Dharmacon. (siGenome On-Target plus; Dharmacon). Negative control siRNA duplex (Stealth RNAi negative control; invitrogen) was used as control. Forward transfection for ATDC5 cells and reverse transfection for primary chondrocytes were carried out using Lipofectamine RNAiMAX reagent (Invitrogen), according to the manufacturer's protocol. In forward transfection, ATDC5 cells were transfected with 50 nM siRNA duplex in regular serum-free culture medium without antibiotics, using Lipofectamine RNAiMAX reagent. After 8 h incubation with the transfection reagent mix, the medium was changed to the differentiation medium with BMP-2 and incubated for 8 days. In reverse transfection, freshly isolated chondrocytes were plated at an initial density of $5x10^4/cm^2$, into the plates that had been coated with Panx3 siRNA-1, siRNA-2 or Stealth RNAi negative control in the presence of Lipofectamine RNAiMAX reagent. After 8 h incubation with the transfection reagent mix, the medium was changed to the differentiation medium with BMP-2 and incubated for 2 days. Expression of *Panx3, Col2a1* and *Col10a1* were analyzed by real time PCR methods.

Measurement of intracellular cAMP— The cells were seeded at 1 X 10^4 cells/well in a 96-well plate and cultured for 7 days with DMEM/F-12 in the presence of 10 μg/ml of ITS. They were then incubated with serum-free 0.1% albumin containing DMEM/F-12 medium for 8–12 hours, followed by exposure to 100 nM rPTH (1-34) for 10 min. The level of cAMP was determined with a Bridge-It cAMP Designer Fluorescence Assay kit (Mediomics). Briefly, the cells were incubated with 50 μl of 1x KRB-IBMX buffer for 15 min at RT and with 50 μl of Forskolin for 15 min at RT. After the solution was removed, the cells were incubated with 100 μl of the cAMP designer assay solution for 30 min while covered with tinfoil to avoid exposure to light. The supernatant was collected and the fluorescence intensity was measured with a plate reader (excitation ~480–485 nm, emission ~520–535 nm).

Measurement of ATP flux

ATP flux was determined by luminometry. To open the pannexin channels, the cells were depolarized by incubation in KGlu solution (140 mM KGlu, 10 mM KCl and 5.0 mM TES, pH 7.5) for 10 min. The supernatant was collected and assayed with luciferase/luciferin (Promega).

RESULTS

Expression of Panx3 in cartilage— While searching for an expression profile of gap junction genes in skeletal tissues through the EST database, we found that *Panx3* was expressed in limbs and cartilage. Because of its unique expression profile and its potential